

# Kondo Effect in Carbon Nanotube Single-Electron Transistors

Eugene H. Kim<sup>1</sup>, Germà Sierra<sup>2</sup>, and C. Kallin<sup>1</sup>

<sup>1</sup> *Department of Physics and Astronomy, McMaster University, Hamilton, Ontario, Canada L8S-4M1*

<sup>2</sup> *Instituto de Matemáticas y Física Fundamental, C.S.I.C., 28006 Madrid, Spain*

Recently, Coulomb blockade physics was observed at room temperature in a carbon nanotube single-electron transistor (H. W. Ch. Postma, *et. al.*, *Science* **293**, 76 (2001)). In this work, we suggest that these devices may be promising for studying the Kondo effect. In particular, they could allow for a detailed investigation of the 2-channel Kondo fixed point. Moreover, fabricating a similar device in a short nanotube could be promising for studying the effect of a magnetic impurity in an ultrasmall metallic grain. Experimental signatures of the Kondo effect in these systems is discussed.

Recently, carbon nanotubes have been the source of an enormous amount of activity. [1] The remarkable control with which these materials can be fabricated and manipulated makes carbon nanotubes an ideal system for studying the electronic properties of one-dimensional conductors. Moreover, these materials are extremely durable, and relatively inexpensive to make. Therefore, besides fundamental science, these systems are promising for commercial applications.

In recent work, [2] a single-electron transistor (SET) was fabricated by introducing two buckles in series in a long single-wall carbon nanotube. The two buckles define a small island (*i.e.* a “quantum dot”) within the nanotube. (See Fig. 1 of Ref. 2). Using this device, the authors of Ref. 2 observed Coulomb blockade physics at room temperature. Moreover, they found that the conductance had a power-law temperature dependence, consistent with a Luttinger liquid model for the leads. In this work, we suggest that this device could be promising for studying the Kondo effect.

The Kondo effect in Coulomb blockade systems has received a considerable amount of attention over the last few years. [3] However, in most of these studies, the leads were described by non-interacting electron gases. The case where the leads themselves are interacting liquids has only recently received attention, and has been shown to exhibit rich behavior driven by these interactions. [4,5] Carbon nanotube SETs could provide a controlled environment for studying the Kondo effect in systems with interacting leads. It should be noted that carbon nanotubes have also been shown to display interesting mesoscopic effects, characteristic of nanoscale conductors. [1] Recently, it has been shown that interesting physics would arise if a magnetic impurity were placed in an ultrasmall metallic grain, due to the finite level spacing of the grain. [6] (In Ref. 6, this system was dubbed the *Kondo box*.) A device similar to the one used in Ref. 2 could provide a controllable realization of the Kondo box.

We begin our discussion by recalling the band structure of carbon nanotubes. These materials consist of a sheet of graphite rolled into a cylinder. A single sheet of graphite consists of carbon atoms arranged on the sites of a honeycomb lattice. The band structure is well described by a tight-binding model with one orbital per lattice site. To form a nanotube, the sheet of graphite is rolled into a cylinder. Doing this quantizes the crystal momentum,

$q_y$ , transverse to the axis of the cylinder. Interestingly, two (one-dimensional) bands of gapless excitations exist at  $q_y = 0$ . The low energy physics is determined by the two bands of gapless excitations (labeled as band-*c* and band-*d*), which disperse with the same velocity.

With regards to interactions, interbranch (*i.e.* backscattering) interactions are weak. These interactions are determined by the short range part of the Coulomb interaction. However, the probability of two electrons being near each other is suppressed in the two low energy bands, since these bands have  $q_y = 0$  and hence are extended around the circumference of the tube. For isolated single-wall nanotubes, however, the Coulomb interaction is unscreened. Therefore, to describe the system in Ref. 2, one must take into account the long range nature of the Coulomb interaction.

A considerable amount is known about the two-band model of interacting electrons. [10] In the undoped case interactions drive the system to a Mott-insulating state, with a gap to both spin and charge excitations. When doped with holes, the spin gap remains and the holes form pairs. In nanotubes, the (backscattering) interactions which drive these instabilities are weak. Hence, these effects will only be observable at very low temperatures/energies. Above the spin gap and pairing energy scale, the system behaves as a Luttinger liquid. [7]

The spin gap introduces complications for the Kondo effect. However, since the spin gap in carbon nanotubes is small, it can be overcome by a modest magnetic field. The main effect of a magnetic field is to shift the bands of the “spin-up” and “spin-down” electrons. Because of this, the processes which cause the spin gap suffer a momentum mismatch and become irrelevant. The only processes which survive are triplet pairing interactions. The results of Ref. 11 suggest that the triplet pairing interactions are marginally relevant, but the energy scale at which their effects are visible is unattainably low. Therefore, we will ignore them. Although the competition of the spin gap and the Kondo effect is an interesting issue, in this work we will focus on the case where there are always low energy spin excitations present.

In Ref. 2, an SET was fabricated by creating a small island within a long single-wall carbon nanotube. Being interested in the low energy properties of the system, we focus on the uppermost level of the island and model it as an Anderson impurity. The Hamiltonian, including the coupling to the leads, is

$$H_{\text{island}} = \varepsilon_0 \sum_s n_s^f + U_0 n_\uparrow^f n_\downarrow^f - \frac{h_0}{2} (n_\uparrow^f - n_\downarrow^f) \quad (1)$$

$$- \sum_{\substack{\lambda=c,d \\ s=\uparrow,\downarrow}} \left( t_{1\lambda} \psi_{1,\lambda,s}^\dagger(0) + t_{2\lambda} \psi_{2,\lambda,s}^\dagger(0) \right) f_s + h.c.,$$

where  $\psi_{i,\lambda,s}$  destroys an electron with spin- $s$  in lead- $i$  ( $i = 1, 2$ ) and band- $\lambda$  ( $\lambda = c, d$ );  $f_s$  destroys an electron with spin- $s$  on the island;  $n_s^f = f_s^\dagger f_s$ ;  $\varepsilon_0$  is the energy level of the island, which can be controlled by a gate voltage;  $U_0$  is the charging energy;  $h_0$  is the magnetic field;  $t_{i\lambda}$  is the matrix element for an electron to tunnel to the island from band- $\lambda$  in lead- $i$ . It is useful to introduce *bonding* and *antibonding* combinations

$$\psi_{i,b,s} = (t_{ic} \psi_{i,c,s} + t_{id} \psi_{i,d,s}) / \sqrt{N_i},$$

$$\psi_{i,a,s} = (t_{id} \psi_{i,c,s} - t_{ic} \psi_{i,d,s}) / \sqrt{N_i}, \quad (2)$$

with  $N_i = t_{ic}^2 + t_{id}^2$ . In terms of these operators, we see that only the bonding combinations couple to the island. Being interested in the Kondo regime, we integrate out charge fluctuations on the island. Working to second order in perturbation theory, [9] we arrive at the effective Hamiltonian

$$H_{\text{int}} = \tau \cdot \frac{\sigma_{s,s'}}{2} \left( J_1 \psi_{1,b,s}^\dagger(0) \psi_{1,b,s'}(0) + 1 \rightarrow 2 \right)$$

$$+ J_{12} \tau \cdot \frac{\sigma_{s,s'}}{2} \left( \psi_{1,b,s}^\dagger(0) \psi_{2,b,s'}(0) + h.c. \right) - h_0 \tau_z, \quad (3)$$

where  $\tau$  is the spin operator for the electron on the island, and the values of the couplings ( $J_i$  and  $J_{12}$ ) can be found in *e.g.* Ref. 4. It is important to note, however, that  $J_i > 0$  and  $J_{12} > 0$ . It should also be noted that in Eq. 3 we have not displayed the potential scattering terms [9] which were generated. For the system considered in this work, these terms have a very small effect and can be ignored. [5]

The dynamics of the leads is described by the Hamiltonian  $H_{\text{leads}} = H_{\text{lead}-1} + H_{\text{lead}-2}$ , where  $H_{\text{lead}-i} = H_i^0 + H_i^1$  is the Hamiltonian for lead- $i$  with [7]

$$H_i^0 = -i v_F \sum_{\lambda,s} \int_{-l}^0 dx \left( \psi_{R,i,\lambda,s}^\dagger \partial_x \psi_{R,i,\lambda,s} - R \rightarrow L \right) \quad (4)$$

$$H_i^1 = U \int_{-l}^0 dx \left( \sum_{\lambda,s} \psi_{R,i,\lambda,s}^\dagger \psi_{R,i,\lambda,s} + \psi_{L,i,\lambda,s}^\dagger \psi_{L,i,\lambda,s} \right)^2.$$

In the above equation,  $\psi_{R,i,\lambda,s}$  ( $\psi_{L,i,\lambda,s}$ ) is the right (left) moving component of  $\psi_{i,\lambda,s}$ . Furthermore, we have followed Ref. 7 and taken the Coulomb interaction to be screened beyond some long distance;  $U$  is the effective strength of this interaction. In the previous paragraph, we saw that only the bonding combination of the fermion fields (Eq. 2) couples to the impurity. Fortunately, we can express the Hamiltonian of the leads in terms of the bonding and antibonding operators as well. In terms of these operators, the Hamiltonian has the same form as Eq. 4, except the labels  $c$  and  $d$  are replaced everywhere by  $b$  and  $a$ .

In what follows, we will make extensive use of the boson representation. To do so, the electron operator is written as  $\psi_{R/L,i,\lambda,s} \sim e^{\pm i \sqrt{4\pi} \phi_{R/L,i,\lambda,s}}$  where the chiral fields,  $\phi_{R,i,\lambda,s}$  and  $\phi_{L,i,\lambda,s}$ , are related to the usual Bose field  $\phi_{i,\lambda,s}$  and its dual field  $\theta_{i,\lambda,s}$  by  $\phi_{i,\lambda,s} = \phi_{R,i,\lambda,s} + \phi_{L,i,\lambda,s}$  and  $\theta_{i,\lambda,s} = \phi_{R,i,\lambda,s} - \phi_{L,i,\lambda,s}$ . It will also prove useful to form *charge* and *spin* fields  $\phi_{i,\lambda,\rho/\sigma} = (\phi_{i,\lambda,\uparrow} \pm \phi_{i,\lambda,\downarrow}) / \sqrt{2}$ , and then form the combinations  $\phi_{i,\rho\pm} = (\phi_{i,b,\rho} \pm \phi_{i,a,\rho}) / \sqrt{2}$  describing *total* and *relative* charge fluctuations in lead- $i$ . In terms of these variables, the Hamiltonian for lead- $i$  is

$$H_{\text{lead}-i} = \frac{v_{\rho^+}}{2} \int_{-l}^0 dx K_{\rho^+} (\partial_x \theta_{i,\rho^+})^2 + \frac{1}{K_{\rho^+}} (\partial_x \phi_{i,\rho^+})^2$$

$$+ \frac{v_F}{2} \int_{-l}^0 dx (\partial_x \theta_{i,\rho^-})^2 + (\partial_x \phi_{i,\rho^-})^2 \quad (5)$$

$$+ \frac{v_F}{2} \sum_{\lambda=b,a} \int_{-l}^0 dx (\partial_x \theta_{i,\lambda,\sigma})^2 + (\partial_x \phi_{i,\lambda,\sigma})^2,$$

where  $K_{\rho^+} = 1/\sqrt{1+8U/(\pi v_F)}$  and  $v_{\rho^+} = v_F/K_{\rho^+}$ . Experimentally, it has been found that  $0.19 \leq K_{\rho^+} \leq 0.26$  for single-wall carbon nanotubes. [2] Finally, to analyze the physics it will prove useful to unfold the system, and work solely in terms of right moving fields. [12]

We begin our discussion of the Kondo effect by considering the case of semi-infinite leads:  $l \rightarrow \infty$ . Near the ultraviolet fixed point, we can compute the conductance using the golden rule. We find  $G \sim T^\alpha$ , where  $\alpha = (1/2)(1/K_{\rho^+} - 1)$ , in agreement with what was reported in Ref. 2. The behavior of the system at lower energies can be deduced by a renormalization group (RG) analysis. To second order in the couplings, [13] the RG equations for the parameters are

$$\frac{d\lambda_+}{dl} = \lambda_+^2 + \lambda_-^2 + g^2, \quad \frac{d\lambda_-}{dl} = 2\lambda_+\lambda_-,$$

$$\frac{dg}{dl} = \frac{1}{4} \left( 1 - \frac{1}{K_{\rho^+}} \right) g + 2g\lambda_+, \quad \frac{d\lambda_h}{dl} = \lambda_h, \quad (6)$$

where  $\lambda_+ \sim (J_1 + J_2)$ ,  $\lambda_- \sim (J_1 - J_2)$ ,  $g \sim J_{12}$ , and  $\lambda_h \sim h_0$ . A few words are in order about the RG equations. Let us first consider  $J_1 = J_2$ , so that  $\lambda_- = 0$ . At the ultraviolet fixed point, the  $J_1$  and  $J_2$  terms are marginally relevant. On the other hand, the  $J_{12}$  term is irrelevant for repulsive interactions ( $K_{\rho^+} < 1$ ). Hence,  $g$  will initially decrease under the RG. For the values of  $K_{\rho^+}$  relevant to this system,  $\lambda_+$  will have grown to  $\mathcal{O}(1)$  while  $g \ll 1$ . [5] If  $g = 0$ , we would have a 2-channel Kondo model, which is known to have a non-trivial  $\mathcal{O}(1)$  fixed point. Therefore, for  $J_1 = J_2$  the low energy physics will be governed by the 2-channel Kondo fixed point with  $g$  (and  $\lambda_h$ ) as perturbations. Now let us consider  $J_1 \neq J_2$ . From Eq. 6,  $\lambda_-$  will grow under the RG. If  $J_1$  and  $J_2$  are considerably different (for concreteness, consider  $J_1 > J_2$ ), the system will flow to the 1-channel Kondo fixed point, where the electron on the island forms a singlet with the electrons in lead-1. [14]

However, for  $J_1 \approx J_2$ ,  $\lambda_-$  will grow slowly, so that the system flows close to the 2-channel Kondo fixed point. In this case, it is appropriate to consider the behavior near the 2-channel Kondo fixed point with  $g$  and  $\lambda_-$  (and  $\lambda_h$ ) as perturbations. Since the device we are considering is made by introducing buckles in a carbon nanotube, it will probably be difficult to achieve  $J_1 = J_2$ . However, as we feel the possibility of observing 2-channel Kondo physics is one of the most interesting features of this system, in what follows we will focus on the case  $J_1 \approx J_2$ . Finally, it should be noted that the magnetic field is a relevant perturbation. Therefore, we must consider very small fields, so as not to completely wipe out the Kondo physics described above.

To analyze the physics near the 2-channel Kondo fixed point, we follow Ref. 16 and form combinations of the fields in the two leads:  $\phi_{R,c}$ ,  $\phi_{R,sp}$ ,  $\phi_{R,f}$ , and  $\phi_{R,sf}$ . Then, we perform the unitary transformation,  $U = \exp(i\sqrt{4\pi} \tau^z \phi_{R,sp}(0))$ , which ties a spin-1/2 from the leads to the island. Finally, we introduce new fermion fields,  $d \sim S^-$  and  $X \sim e^{i\sqrt{4\pi}\phi_{R,sf}}$ . Upon performing these transformations,  $H_{\text{int}}$  becomes

$$\begin{aligned} H_{\text{int}} = & v_F \lambda'_+ (d^\dagger - d) (X^\dagger(0) + X(0)) \\ & + v_F \lambda'_- (d^\dagger + d) (X^\dagger(0) - X(0)) - v_F \lambda'_h (d^\dagger d - 1/2) \\ & + v_F g' (d^\dagger + d) \left( e^{-i\sqrt{4\pi}\phi_{R,f}(0)} - e^{i\sqrt{4\pi}\phi_{R,f}(0)} \right), \end{aligned} \quad (7)$$

where  $\lambda'_+$ ,  $\lambda'_-$ ,  $g'$ , and  $\lambda'_h$  are the renormalized values of the couplings. Note that in Eq. 7, we have displayed only the most relevant operators. A few words are in order about Eq. 7. To begin with, the  $\lambda'_+$  term sets the 2-channel Kondo energy scale; the  $g'$ ,  $\lambda'_-$ , and  $\lambda'_h$  terms are perturbations about the 2-channel Kondo fixed point. The  $g'$  term has dimension  $(1 + 1/K_{\rho+})/4$ , and is relevant for  $K_{\rho+} > 1/3$ . Hence, this term is irrelevant for the system we are considering. Both the  $\lambda'_-$  and  $\lambda'_h$  terms have dimension 1/2 and are relevant. If these terms are absent, the zero temperature fixed point would be the 2-channel Kondo fixed point. However, nonzero  $\lambda'_-$  and/or  $\lambda'_h$  drives the system away from the two-channel Kondo fixed point.  $\lambda'_-$  drives the system to the 1-channel Kondo fixed point, where the electron on the island forms a singlet with the electrons in the lead with the larger exchange coupling. [14,15] The  $\lambda'_h$  term drives the system to a fixed point where the electron on the island is spin polarized; spin-flip processes are energetically costly, and the electron on the island behaves as a potential scatterer. [15] The energy scale at which 2-channel Kondo behavior will no longer be observable is determined by the values of  $\lambda'_-$  and  $\lambda'_h$ .

Signatures of the 2-channel Kondo fixed point can be observed in conductance measurements. Using the golden rule, we find

$$\begin{aligned} G/G_0 = & \frac{1}{\Gamma(\beta)} \left( \frac{T}{T_K} \right)^{\beta-2} \int \frac{dx}{2\pi} \operatorname{sech}^2 \left( \frac{x T_K}{2T} \right) \\ & \times \left| \Gamma \left( \frac{\beta}{2} + i \frac{x T_K}{2\pi T} \right) \right|^2 \frac{\Gamma_-(1+x^2) + \Gamma_h}{(x^2 - \Gamma_h - \Gamma_-)^2 + x^2(1 + \Gamma_-)^2}. \end{aligned} \quad (8)$$

In Eq. 8,  $T_K = E_0 \exp(-1/\lambda_+)$ , where  $E_0$  is a high-energy cut-off;  $\beta = (1/2)(1 + 1/K_{\rho+})$ ;  $G_0 = (2e^2/h)(g')^2/(2\pi)$ ;  $\Gamma_- \sim (\lambda'_-)^2$ ;  $\Gamma_h \sim (\lambda'_h)^2$ .  $G/G_0$  vs.  $T/T_K$  is plotted in Fig. 1 for several values of  $K_{\rho+}$ . To begin with, notice that the conductance decreases as the temperature is decreased. This should be contrasted with the case of non-interacting leads, where the Kondo effect leads to perfect conductance at low temperatures. [3] This behavior is due to the interactions in the leads. From Eq. 8, it follows that  $G \sim T^{\beta-2}$  for  $\Gamma_h, \Gamma_- \ll T \ll T_K$ . This temperature dependence is a property of the 2-channel Kondo fixed point. However, for  $T < \Gamma_-$  and/or  $T < \Gamma_h$ , the system is far from the 2-channel Kondo fixed point, and the temperature dependence is modified from its 2-channel Kondo behavior.

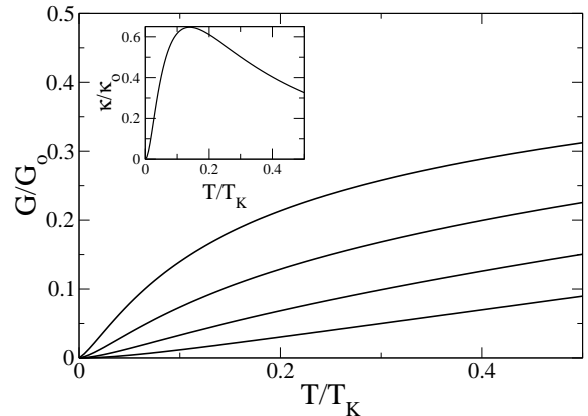


FIG. 1.  $G/G_0$  vs.  $T/T_K$  near the 2-channel Kondo fixed point.  $K_{\rho} = 0.29, 0.26, 0.23, 0.2$  in order from the top to the bottom curve. Inset:  $\kappa/\kappa_0$  vs.  $T/T_K$  near the 2-channel Kondo fixed point. In both plots, the parameters  $\Gamma_-$  and  $\Gamma_h$  were taken to be  $\Gamma_- = 0.07$  and  $\Gamma_h = 0.1$ .

Besides the (charge) conductance, 2-channel Kondo physics can also be observed in thermal conductance measurements. An interesting property of the 2-channel Kondo fixed point is that it has perfect spin conductance. [5] Though the spin conductance is difficult to measure, this will manifest itself in the thermal conductance — as charge transport is suppressed, the thermal conductance will be dominated by spin. Computing the thermal conductance [17] due to spin, we find

$$\begin{aligned} \kappa/\kappa_0 = & \left( \frac{3}{4\pi^2} \right) \left( \frac{T_K}{T} \right)^3 \int dx \operatorname{sech}^2 \left( \frac{x T_K}{2T} \right) \\ & \times \frac{x^4(1 - \Gamma_-)^2}{(x^2 - \Gamma_h - \Gamma_-)^2 + x^2(1 + \Gamma_-)^2}, \end{aligned} \quad (9)$$

where  $\kappa_0 = (\pi^2/3)T/h$  is the value for perfect thermal conductance.  $\kappa/\kappa_0$  vs.  $T/T_K$  is shown in the inset of Fig. 1. From Eq. 9,  $\kappa \rightarrow \kappa_0$  for  $\Gamma_h, \Gamma_- \rightarrow 0$  (for  $T \ll T_K$ ). This is due to the perfect spin conductance of the 2-channel Kondo fixed point. However,  $\Gamma_- \neq 0$  and/or  $\Gamma_h \neq 0$  drives the system away from the 2-channel Kondo fixed point and destroys the perfect spin conductance.

Another way to probe the Kondo physics is by measuring the differential capacitance as a function of gate

voltage. [18] At  $T = 0$ ,  $C = \partial^2 E_G / \partial V_G^2$ , where  $E_G$  is the ground-state energy and  $V_G$  is the gate voltage coupled to the island. Furthermore, we expect  $\varepsilon_0 = \eta V_G + \text{const}$ , where  $\eta$  is a constant. For  $\Gamma_-, \Gamma_h \ll T_K$ , the contribution to the ground state energy due to the Kondo effect is  $\delta E_G \approx (\ln(c_0)/2\pi) T_K$ , where  $c_0$  is a constant of order unity. Differentiating, we find

$$C \sim \varepsilon_0^2 \exp\left(\frac{\pi \varepsilon_0 (\varepsilon_0 + U_0)}{U_0 \Gamma_0}\right), \quad (10)$$

where  $\Gamma_0 = 2(t_{1c}^2 + t_{1d}^2 + t_{2c}^2 + t_{2d}^2)/v_F$ . This strongly varying function of gate voltage is due to the Kondo effect. The differential capacitance vs. gate voltage is plotted in Fig. 2.

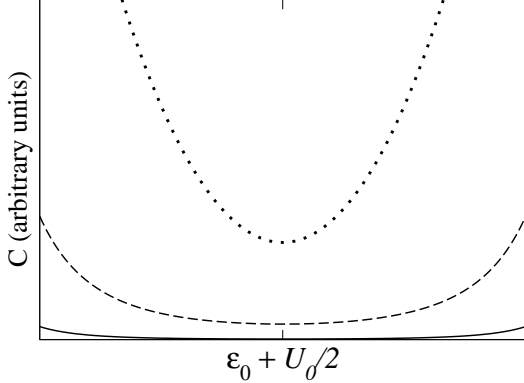


FIG. 2. Differential capacitance vs. gate voltage — dotted line: island coupled to semi-infinite leads; dashed line: Kondo box with  $N = \text{even}$ ; solid line: Kondo box with  $N = \text{odd}$ .

Now we consider the Kondo effect in a short nanotube — a Kondo box. More specifically, we consider a short carbon nanotube with a buckle introduced near one of the ends. This buckle defines a small island, which is connected to a larger nanotube “nanoparticle” of length  $l$ . (See Fig. 3.) For this configuration,  $t_{2c} = t_{2d} = 0$  in Eq. 1. Also, to simplify things let us consider  $h_0 = 0$ . Then, only  $J_1 \neq 0$  while  $J_2 = 0$  and  $J_{12} = 0$  in Eq. 3. The Kondo effect in this system can be probed by measuring the differential capacitance as a function of gate voltage. Here, we find that the results strongly depend on the total number of particles in the system,  $N$ . ( $N = \text{number of electrons in the nanoparticle} + \text{electron on the island}$ .) Calculating the shift in the ground state energy, we find

$$\begin{aligned} \delta E_G &= -\frac{3}{4} \frac{\Delta}{\ln\left(\frac{\Delta}{T_K}\right)} & N = \text{even}, \\ \delta E_G &= -\frac{2.7}{160} \frac{\Delta}{\ln^2\left(\frac{\Delta}{T_K}\right)} & N = \text{odd}, \end{aligned} \quad (11)$$

where  $\Delta = v_F \pi / l$  is the level spacing, and we are assuming  $T_K \ll \Delta$ . Notice that  $\delta E_G$  is significantly greater for  $N = \text{even}$  as compared with  $N = \text{odd}$ . This occurs because for  $N = \text{even}$ , the ground state of the nanoparticle has spin=1/2; the free spin in the nanoparticle can

form a singlet with the electron on the island. However, for  $N = \text{odd}$  the nanoparticle has a singlet ground state; the coupling between the nanoparticle and the island is through virtual fluctuations. The differential capacitance vs. gate voltage is plotted in Fig. 2

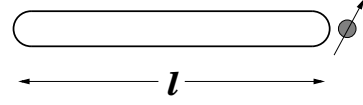


FIG. 3. Schematic of the Kondo box configuration: a small island coupled to a larger nanotube “nanoparticle”.

In conclusion, carbon nanotube SETs [2] may be promising for studying the Kondo effect. With semi-infinite leads, this system allows for a detailed investigation of the 2-channel Kondo fixed point. We also considered the Kondo effect in a finite-sized nanotube — a Kondo box. Here, we saw that the results depend on whether the total number of particles is even or odd. Finally, it is worth noting that generalizations of this device could allow for the study of other related phenomena. For example, introducing two islands in the nanotube could allow one to study two-impurity Kondo physics, or more generally, the properties of coupled quantum dots.

EHK is grateful to H. Paik for bringing Ref. 2 to his attention. This work was supported by the NSERC of Canada (EHK and CK), and the Spanish grant PB98-0685 (GS).

- 
- [1] For reviews, see C. Dekker, *Physics Today* **52**(5), 22 (1999); *Physics World* **13**(6) (2000).
  - [2] H. W. Ch. Postma, *et. al.*, *Science* **293**, 76 (2001).
  - [3] For a review, see L. Kouwenhoven and L. Glazman, *Physics World* **14**(1), 33 (2001).
  - [4] P. Simon and I. Affleck, *Phys. Rev. B* **64**, 85308 (2001).
  - [5] E. H. Kim, cond-mat/0106575.
  - [6] W. B. Thimm, J. Kroha, and J. von Delft, *Phys. Rev. Lett.* **82**, 2143 (1999).
  - [7] C. L. Kane, L. Balents, and M. P. A. Fisher, *Phys. Rev. Lett.* **79**, 5086 (1997).
  - [8] R. Egger and A. O. Gogolin, *Phys. Rev. Lett.* **79**, 5082 (1997).
  - [9] J. R. Schrieffer and P. A. Wolff, *Phys. Rev.* **149**, 491 (1966).
  - [10] See, for example, H-H. Lin, L. Balents, and M. P. A. Fisher, *Phys. Rev. B* **56**, 6569 (1997), and references therein.
  - [11] D. C. Cabra, *et. al.*, cond-mat/0012235.
  - [12] S. Eggert and I. Affleck, *Phys. Rev. B* **46**, 10866 (1992).
  - [13] J. Cardy, *Scaling and Renormalization in Statistical Physics*, (Cambridge University Press, Cambridge, 1996).
  - [14] P. Nozieres and Blandin, *J. Phys. (Paris)* **41**, 193 (1980).
  - [15] I. Affleck, *et. al.*, *Phys. Rev. B* **45**, 7918 (1992).
  - [16] A. Schiller and S. Hershfield, *Phys. Rev. B* **51**, R12896 (1995); K. Majumdar, A. Schiller, and S. Hershfield, *ibid* **57**, 2991 (1998).
  - [17] U. Sivan and Y. Imry, *Phys. Rev. B* **33**, 551 (1986).
  - [18] D. Berman, *et. al.*, *Phys. Rev. Lett.* **82**, 161 (1999).